Aspects of the Target Voltage Behavior in Reactive Sputtering

R. De Gryse, D. Depla, and J. Haemers, Ghent University, Ghent, Belgium

Key Words: Reactive sputtering, Target voltage, Subplantation, Plasma

ABSTRACT

Over the last couple of years, more and more evidence has become available [2,3,9] which shows that at least two mechanisms are responsible for target poisoning during reactive sputtering, i.e. subplantation of the reactive gas ions underneath the target surface and the well known mechanism of chemisorption [1] on the target surface. At first sight, both processes may look quite similar, however, their influence on the target poisoning is very different. Also with respect to the absolute target voltage (ATV) behavior, the differences are very pronounced. The reason for these differences finds its origin in the fact that subplanted species can react with the target metal and form compound molecules, or can remain unreacted as dissolved reaction gas in the target. Which path will be followed largely depends on factors such as reactivity between implanted species in the host lattice and diffusivity in the already formed compound environment. In systems with Al as a target material and oxygen as reaction gas, high reactivity is expected and little or no dissolved and free oxygen atoms will survive in the Al target lattice. However, as soon as poisoning starts and the target subsurface is converted into oxide, reactivity is no longer the dominant factor but the diffusivity of oxygen in the oxide determines the "equilibrium" or steady state amount of dissolved oxygen in the target subsurface. In systems with a low inherent reactivity such as Si/N_2, compound formation by reaction with the molecular gas is less pronounced and considerable amounts of nitrogen will become dissolved in the subsurface during the poisoning process. Stopping the magnetron discharge allows one to measure the nitrogen emanating from the target [3,5].

The formed compound, for instance the oxide, at the target surface and subsurface behaves completely different with respect to the ATV as compared to target material onto which reaction gas has been chemisorbed. This has to do with the difference between the ion induced secondary electron emission (ISEE) coefficient of the formed oxide as compared to the ISEE coefficient of the target material partly covered with chemisorbed oxygen. Moreover, chemisorption of oxygen on previously formed oxide, either grown by subplantation or by classic oxidation, has a reduced probability.

A model is discussed in which the ATV is expressed as the weighted difference between the fraction of the target surface area occupied by chemisorbed species and the fraction of the target surface which is converted into compound by ion implantation. This model is used to understand the ATV behavior during reactive sputtering of aluminium in an argon/oxygen mixture. It is shown that the frequently observed increase in ATV before the poisoning transition occurs is due to chemisorption. On the contrary, the abrupt decrease in ATV upon poisoning is essentially due to the compound formation by subplantation.

In systems such as Nb/O_2, Sn/N_2, Si/N_2, etc., the ATV is reported to increase upon poisoning. Up to now, no satisfactory explanation has been given for this effect. It will be shown that unreacted and dissolved reaction gas in the target can give rise to such a behavior. N_2^+ ions were implanted in situ in Ag targets which afterwards were used in a sputter experiment. It was observed that the implantation of N_2^+ ions results in an increase of the ATV. Under the given circumstances, Ag and N do not react chemically, which leads to the conclusion that dissolved reaction gas can be responsible for an increase in ATV when poisoning occurs.

INTRODUCTION

In reactive sputtering, the target voltage is essentially controlled by two effects, namely a plasma effect and the variation of the Ion-induced Secondary Electron Emission (ISEE) coefficient. The first effect has to do with the variation of the plasma impedance under the influence of variations in sputter partial pressures of the sputter gas and reactive gas when going from metallic sputtering toward poisoning. The second and dominating effect is due to the formation of a compound layer at the target surface, a compound layer which has a different ISEE value as compared to the original target surface. While the first effect leads to a gradual decrease of the target voltage, the ISEE-effect is characterized by abrupt variations of the target voltage in a narrow region of pressure or flow variations. This article will essentially focus on the effect of the ISEE-coefficient on the absolute target voltage (ATV).

505/856-7188
48th Annual Technical Conference Proceedings (2005) ISSN 0737-5921

During the reactive sputtering process, the partial pressure of the reactive gas is lowered by the chemical reaction between the reactive gas and the sputtered target material. This is the so-called gettering process. This process is generally described by chemisorption of the reactive gas on the target material deposited on the substrate and the chamber walls [1]. Of course, this reaction can also occur on the target, but there it is balanced by the sputtering process. The balance between sputtering and chemical reaction on the target shifts towards more chemical reaction when the flow rate of the reactive gas exceeds the getter rate. This reduces the erosion rate of the target because the formed compound sputters less efficiently than the original target material. Consequently, the getter rate reduces further which results in an avalanche situation and an abrupt change in the partial pressure of the reactive gas, which is mostly accompanied with an abrupt change in target voltage and deposition rate. This description of the reactive sputtering process is summarized in the model of Berg et al. [1]. As shown by the authors [2], even for reactive gas/target combinations where gettering plays an important role, i.e. O_2/Al, chemisorption alone cannot explain the measured target voltage behavior. Ion implantation also plays an important role in the poisoning mechanism during the reactive sputtering process. A model was put forward [9] in which chemisorption as well as ion implantation were combined.

Based on this model it is shown that the variation in ATV in the system Al/O_2, when driving the target in poisoning, can be simulated with good accuracy by using the difference between the effective fraction of the target covered by chemisorption θ^*_{tc} and the fraction θ_{ti} of the target surface that has reacted with the subplanted reactive atoms under the formation of compound. It follows that chemisorption is essentially the trigger for reactive implantation which drives the target in full poisoning. In the system, Al/O_2 like in several others, the ATV shows a sharp drop upon poisoning. In many systems, however, systems such as Nb/O_2, Sn/N_2, Si/N_2, etc., the ATV is increasing upon poisoning. For the time being this behavior is not well understood and part of this paper concerns this particular effect. It will be shown that reactive ion implantation is liable to explain such a behavior. For simplicity and for studying this effect we will focus on the system Ag/N_2 which gives rise to a pronounced increase in ATV, even in metallic mode and without the formation of any compound.

EXPERIMENT

The experimental conditions have been previously described in detail [3,8]. The same setup was used for the target voltage experiments. However, to investigate the influence of the pumping speed, a valve was introduced between the vacuum chamber and the turbomolecular pump. We have used a Hüttinger 1500 DC power supply in constant current mode. The pumping speed was measured by using the ratio between the measured flow (MKS type 246) and the measured argon pressure (MKS Baratron).

OVERVIEW OF THE MODEL

Figure 1 gives a schematic overview of the extended model. Similar to the model proposed by Berg et al. [1] we define three reactive gas flows : i) the reactive gas flow to the target q_t; ii) the reactive gas flow to the substrate q_s, and iii) the reactive gas flow to the pump q_p. The total of these flows is equal to the reactive gas flow introduced in the chamber, q_o. The reactive gas molecules can chemisorb on the substrate (and chamber walls), resulting in a given fraction θ_{sc} of the substrate which has reacted. The reactive gas ions become implanted into the target, resulting in a given degree of reaction for the target θ_{ti}, as described in the first part of the paper. On the non-reacted part of the target ($1-\theta_{ti}$), reactive gas molecules can chemisorb on the target surface, resulting in an effective fraction of the target covered by chemisorbed molecules.

$$\theta^*_{tc} = \theta_{tc}(1-\theta_{ti}) \qquad \text{Equation 1}$$

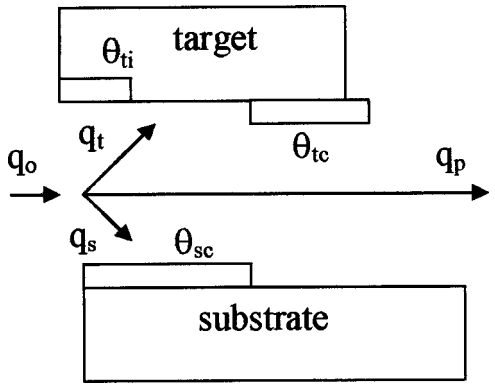

Figure 1. Overview of the extended model. See text for a detailed description of the different symbols.

Without going into the mathematical details [9] and assuming steady state conditions, the extended model is governed by a set of equations given in the appendix. It follows that starting from experimental values of the discharge current density I, the total gas pressure P_T and the partial pressure P of the reaction gas, all relevant quantities pertaining to the target can be calculated. At the substrate and chamber walls only chemisorption is the mechanism at play and has been fully documented by Berg et al. [1]. The variation in time of the chemisorbed fraction on the substrate (and walls) θ_{sc} is given by

$$n_{opp}\frac{d\theta_{sc}}{dt}=\frac{2\alpha_{sc}}{a}(1-\theta_{sc})F + I\gamma_R\left[(1-\theta_{ti})\theta_{tc}+\theta_{ti}\left(\frac{n_o}{n_o+N}\right)\right](1-\theta_{sc})\frac{A_t}{A_s} - I\gamma_M(1-\theta_{ti})(1-\theta_{tc})\left(\frac{n_o}{n_o+N}\right)\theta_{sc}\frac{A_t}{A_s}$$

Equation 9

with A_t and A_s the respective areas of target racetrack and substrate, α_{sc} the sticking coefficient of the reaction gas on the freshly deposited target material and n_{opp} the target surface density. It should be noted that the influence of shallow implantation on the target is taken into account by the factors containing θ_{ti} and $(1 - \theta_{ti})$. In steady state conditions the left hand side of Equation 9 equals zero which allows one to calculate θ_{sc} which in turn gives access to the respective gas flows towards substrate and target.

$$q_s=\frac{RT}{N_a}\alpha_{sc}(1-\theta_{sc})F.A_s$$

Equation 10

$$q_t=\frac{RT}{N_a}\alpha_{tc}(1-\theta_{tc})(1-\theta_{ti})FA_t+\frac{fI}{N_a}RTA_t$$

Equation 11

Taking into account the gas flow transferred by the pump

$$q_p=P.S$$

Equation 12

with S the pumping speed, the total gas flow q_o of the reaction gas is given by

$$q_o=q_p+q_s+q_t$$

Equation 13

and allows us to discuss variations of ATV as a function of the flow of reaction gas. In the following paragraph we will first discuss the different parameters needed for describing the system Al/O_2, i.e. aluminium sputtered reactively in a mixture of Argon and oxygen. For the pumping speed S and the ion current density I, the experimental values described in Figures 2 and 3 were used. Also the experimental value of the argon pressure (0.2 Pa) was used. The racetrack area A_t (10^{-2} m^2) was measured from a sputtered target. We have set the substrate surface area (and chamber walls) A_s to 1 m^2. We have assumed that the formed compound on the target by ion implantation or chemisorption is Al_2O_3, i.e. a = 1.5. The sputter yield for Al (0.5) was calculated from SRIM 2000.40 [4]. For the sputter yield of Al_2O_3 we have used the experimental value of 0.03 [5]. In our calculation, we have neglected the weighting of the sputter yield by the mole fraction f for the bombardment by Ar^+ and R_2^+ ions because for the performed experiments (see further) the reactive gas mole fraction in the plasma is always small.

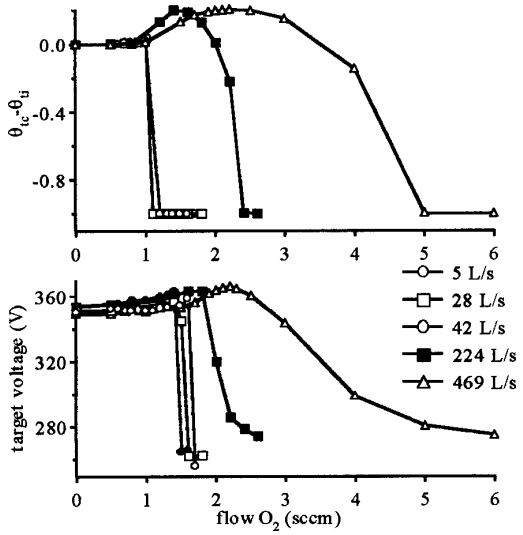

Figure 2. (a) Behavior of the target condition as a function of the oxygen flow using the parameters described in the text. (b) Behavior of the target voltage as a function of oxygen flow. For these experiments the current was kept constant at 200 mA and the pumping speed was varied. The argon pressure was kept constant for all experiments at 0.2 Pa and oxygen was added to the plasma.

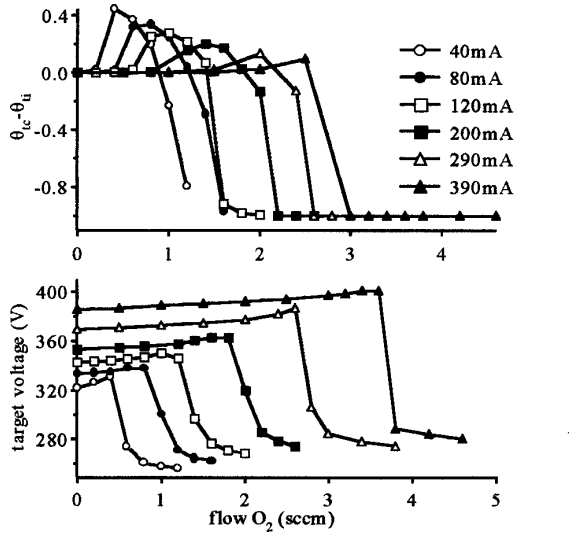

Figure 3. (a) Behavior of the target condition as a function of the oxygen flow using the parameters described in the text. (b) Behavior of the target voltage as a function of the oxygen flux. For these experiments the pumping speed was kept constant at 224 L/s. The argon pressure was kept constant for all experiments at 0.2 Pa and oxygen was added to the plasma.

The reaction probability α_{ti} has been set equal to 1 as it is generally accepted that the implanted oxygen atoms have a high affinity for the target material. As shown by the authors [2] there is evidence for the presence of non-reacted oxygen in the target before complete poisoning. As was discussed [9], this can be attributed to the high current density used during magnetron sputtering. Indeed, at this high current density the rate-determining step in the reaction is not the supply of oxygen atoms to the target, as is the case during ion beam experiments. Therefore, when the target is partially poisoned, some of the oxygen can remain in the target without chemical reaction. As shown by the authors [2], when the magnetron is switched off, these non-reacted oxygen atoms will react further with the target material or desorb from the target as oxygen molecules. We have used the same values for β and N_{max} as in the case of Si/N_2 [9], although no experimental evidence for these values can be given. However, and as mentioned before, the value of β and N_{max} does not affect the general behavior of the calculated results.

From the simulations, we have noticed that the most important parameters are the sticking coefficients needed to describe the chemisorption on the target and the substrate. A best fit between the experimental target voltage curves and the calculated ones (see further) has been achieved using a value of 0.03 and 0.2, respectively, for the sticking coefficient on the target α_{tc} and on the substrate α_{sc}. The higher sticking coefficient for chemisorption on the substrate than on the target can be attributed to the higher activity of the deposited aluminium. A similar reasoning has been used to explain the higher sticking coefficient on freshly evaporated Ti films [6]. The sticking coefficient on the substrate is in the same order of magnitude as the reported sticking coefficient reported by Kusano et al on Ti substrates during reactive sputtering of Ti in Ar/O2 [6]. The sticking coefficient on the target is 10 times larger than the value of the sticking coefficient (0.003) as measured by the authors for O_2 on a freshly sputtered target [5]. However, in the latter situation the sticking coefficient was measured in the power-off mode of the magnetron. As shown by Pekker [7], the dissociation of molecular oxygen in the plasma during magnetron sputtering can be significant. As the produced oxygen atoms have a high sticking coefficient on aluminium, the average sticking coefficient will be larger than the sticking coefficient for molecular oxygen on the aluminium target and will depend on the degree of dissociation of the molecular oxygen. As the degree of dissociation of molecular oxygen is small before full oxidation of the target, or under conditions of high pumping speed [7], the used value of the sticking coefficient is reasonable.

Most published models assume for the sticking coefficient on the target α_{tc} and on the substrate α_{sc} a value of 1. This value can only be reached under reactive sputtering conditions where the degree of dissociation of the molecular gas is very high [7]. In our approach we assume that the bombardment of the target with the reactive gas ions depends linearly on the mole fraction of the reactive gas in the plasma, neglecting the plasma chemistry.

SIMULATION OF THE ABSOLUTE TARGET VOLTAGE (ATV) IN THE SYSTEM Al/O_2

To describe the target voltage behavior as a function of the oxygen flow, the influence of the different poisoning mechanisms, i.e. chemisorption and reactive ion implantation on the target voltage must be known. It is generally accepted that Al_2O_3 has a larger ISEE coefficient than Al. Therefore, the formation of bulk oxide due to reactive ion implantation will influence the target voltage. An increase of the ISEE coefficient of the target will result in a smaller absolute value of the target voltage when the current is kept constant. As shown by the authors, chemisorption of oxygen on an aluminium target [2,5], reduces the ISEE coefficient and is accompanied by an increase of the absolute target voltage until one monolayer of oxygen is chemisorbed. Therefore, we have used the sum $(w_{tc}\theta_{tc}^{*}-w_{tc}\theta_{ti})$ to compare the calculated values with the measured target voltage behavior. In this sum w_{tc} and w_{ti} represent two weighting coefficients which have been set to 1 as no data is available on the magnitude of the target voltage decrease due to bulk oxidation by ion implantation. θ_{tc}^{*} represent the effective fraction of the target covered by chemisorption and is calculated from Figure 1 and, as discussed before, results in an increase of the absolute target voltage.

The target voltage will also decrease by the sudden pressure increase when the gettering of oxygen is reduced. However, this sudden pressure increase is always accompanied with the full oxidation of the target, which is described by θ_{ti}, and in this way this effect has already been taken into account. In Figures 2 and 3 we show the target voltage behavior as a function of the oxygen flow for two different experimental series'. In this first series, we have varied the pumping speed while in the second series the current was varied. Also, the calculated values of $(w_{tc}\theta_{tc}^{*}-w_{ti}\theta_{ti})$ (with $w_{tc} = w_{ti}=1$) are shown. In both series' we notice that the calculated results show a similar behavior as the experimental results. The experiments show that the small target voltage rise, noticed before the abrupt drop of the target voltage, becomes smaller for lower pumping speeds and higher currents. This behavior is reflected by the calculations. Figure 4 shows the behavior of both q_{tc}^{*} and q_{ti}, a function of the oxygen flow for two different pumping speeds. This figure clearly demonstrates that the target voltage must increase due to chemisorption and then will decrease due to the bulk oxidation by reactive ion implantation. The effect is much more pronounced at high pumping speed than at low pumping speed.

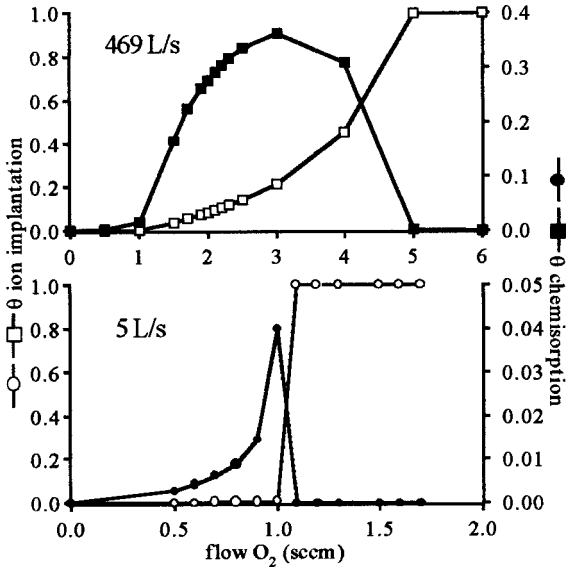

Figure 4. θ^*_{tc} (closed symbols, right hand axis) and (open symbols left hand axis) as a unction of the oxygen flow (different X-axis scale) for two different pumping speeds (and constant current of 200 mA).

This behavior of the target condition can be understood as follows. When the flow rate of the reactive gas exceeds the getter rate at approximately 1 sccm of reactive gas, the effective reactive gas partial pressure starts to increase. At high pumping speed (or at low current) this pressure increase is quite small in contrast to the low pumping speed (or high current) experiments. Therefore, the reactive gas mole fraction f is quite small. As chemisorption is directly proportional with the partial pressure (see Equation 7), chemisorption initially plays a more important role than reactive ion implantation (which is strongly related to f) in the poisoning mechanism. The chemisorption of reactive gas on the target surface reduces, however, the target surface recession speed or the erosion rate of the target. In this way, reactive ion implantation becomes more pronounced. As the reactive gas does not chemisorbs on the reacted target surface, the effect of chemisorption is reduced. At low pumping speed (or high current) the increase of the reactive gas partial pressure is much stronger and in this way the reactive gas mole fraction becomes large enough to fully oxidize the target by reactive ion implantation.

XPS MEASUREMENTS ON Ag-TARGETS

We performed three XPS measurements (see Figure 5) on a fresh Ag target.

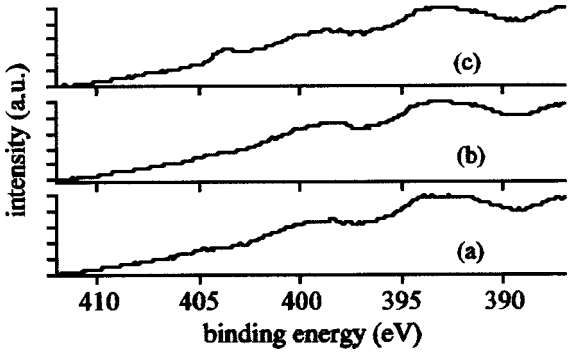

Figure 5. XPS spectra: (a) after Ar sputter cleaning; (b) after nitrogen gas exposure; (c) after nitrogen implantation.

First the target was sputter cleaned using Ar (2 keV). The XPS spectrum reveals two small peaks at binding energy of approximately 392 eV and 397 eV. These peaks can be attributed to distinct peaks in the loss function of silver [10-11]. After pumping the argon form the XPS chamber, we introduced nitrogen ($5x10^{-6}$ Pa) for 25 minutes and recorded simultaneously the same binding energy interval as in experiment 1. No difference in the XPS spectrum was noticed which let us conclude that chemisorption of N_2 at room temperature is negligible. In a third experiment, after sputtering with argon, the target was sputtered with N_2^+ ions (2 keV) for 25 minutes and the XPS spectra were simultaneously recorded. We noticed an extra peak at a binding energy of 403.5 eV while no other differences are noticed. Following Gouzman et al. [12] this peak can be attributed to N_2 molecules physically trapped in a silver matrix. These molecules should originate from recombination of N atoms, as the used ion energy (2 keV) is sufficiently high to overcome the dissociation energy of N_2 (9.8 eV) during ion implantation. A similar effect was noticed during the glow discharge sputtering of Cu in an argon/nitrogen plasma [13]. From these experiments it follows that no Ag-N compounds are formed upon implantation of nitrogen into silver or by chemisorption. So none of the nitrogen species in the plasma can result in the formation of a target surface compound. However, the implanted nitrogen is identified as molecular nitrogen dissolved in the silver matrix. So, the $Ag/N_2/Ar$ system is essentially a non-reactive sputtering system. In this way, it forms an excellent system to study the influence of nitrogen addition on the target voltage during the reactive sputtering process in the metallic mode.

ION IMPLANTATION EXPERIMENTS IN THE DEPOSITION CHAMBER

After sputter cleaning the target in pure argon until the target voltage remains constant, the magnetron was switched off and nitrogen introduced into the deposition chamber (0.05 Pa). Then the ion gun was switched on. After increasing the emission current to 20 mA and setting the ion energy to 5 keV, the shutter between the ion gun and the magnetron was

opened. Meanwhile the magnetron remained in the power-off mode. In this way we could expose the target to a certain N_2^+ ion dose. After a given exposure, the shutter was closed and the ion gun switched off. The nitrogen gas was evacuated from the chamber and argon introduced (0.4 Pa). Then the magnetron was switched on and the target voltage registered. The waiting time between closing the shutter and switching on the magnetron was 20 s. In a first series of experiments, we have registered the target voltage in this way for different ion doses. As can be concluded from Figure 6a, increasing the ion dose results in a target voltage increase. Also, it takes more time to return to the metallic target voltage as the ion dose is increased.

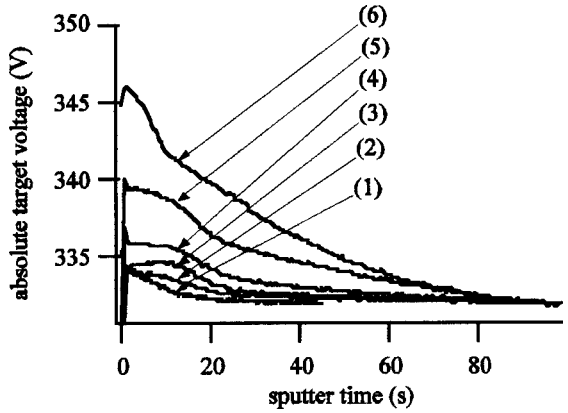

Figure 6a. Influence of ion implantation on the ATV. Influence of the ion exposure (1) 2h; (2) 4h; (3) 8h; (4) 16h; (5) 32h; (6) 64s. (The sharp lines at the beginning of the measurements are due to arcing).

In a second series of experiments (Figure 6b), the ion dose, i.e. the exposure time, was kept constant. However, the waiting time between the end of the ion exposure and the switching on of the magnetron was increased. After a waiting time of 100 s, no effect of the ion implantation on the target voltage is noticed. After switching on the magnetron after a waiting period of 100 s, the target voltage remains constant at the value of metallic silver sputtering. From this experiment, we can conclude that the ion implantation effect on the target voltage is not constant in time and decreases if a waiting period is introduced between the ion exposure and subsequent magnetron sputtering. As the exposure time is long due to the low ion current density, residual gas effects can eventually interfere with the effect of the ion implantation. To exclude residual gas effects on the target voltage, we have also measured the target voltage behavior after 48 h under conditions identical to those during the ion implantation experiment, but without the use of the ion gun. No influence on the target voltage was noticed. Also, no influence on the target voltage was measured if the implantation was performed with argon ions instead of nitrogen ions. From the foregoing measurements one can already conclude that molecular nitrogen, N_2, dissolved in the lattice of a silver target, give rise to an increase of the absolute target voltage. From the waiting experiments it follows that the dissolved nitrogen diffuses out of the target in less than 100 s. Similar results have been observed when using a silicon target sputtered in a mixture of argon and nitrogen [3]. The outdiffusion of N_2 could be monitored with a mass spectrometer. The fact that no variation in target voltage is observed when nitrogen is replaced by argon in the implantation experiments could then be ascribed to the much faster outdiffusion of implanted argon out of the silver target lattice. In other words, during the delay period between implantation of argon and starting the magnetron, all implanted argon has already disappeared.

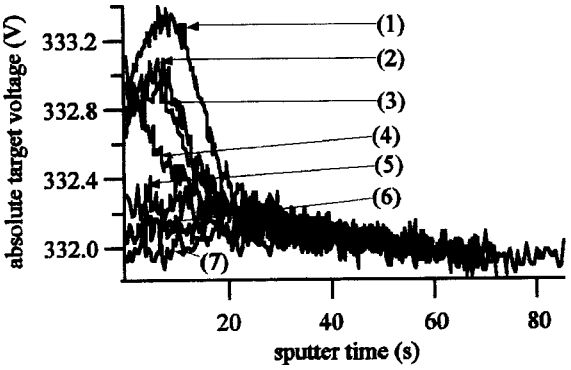

Figure 6b. Influence of ion implantation on the ATV. Influence of the waiting period between exposure and subsequent sputtering (1) 20s; (2) 25s; (3) 30s; (4) 40s; (5) 50s; (6) 80s and (7) 100s.

As shown by the nitrogen ion implantation experiments, the target voltage is clearly influenced by nitrogen ion implantation. As magnetron sputtering during all the ion implantation experiments was performed under identical conditions, this effect must be attributed to a change of the ion induced secondary electron emission (ISEE) coefficient of the target. Implantation of nitrogen ions in the target seems to reduce the ISEE coefficient, and consequently increases the impedance of the system, resulting in a target voltage increase at constant power. Based on the XPS measurements, we may conclude that this ISEE coefficient change is not related to the formation of a silver compound, but is due to the presence of a given concentration of nitrogen atoms or molecules in the silver target. This concentration depends on the N_2 desorption from the target and the target sputter rate (host lattice sputtering). Indeed, as shown by Tsai [14] and Liebl [15], simultaneous sputtering and ion implantation results in an equilibrium concentration of implanted ions in the top layer of the target. The thickness of the top layer depends on the ion range and the maximum equilibrium concentration is inversely proportional to the sputter rate of the target. The effective concentration will be lower if desorption cannot be neglected, which is clearly the case in our experiments as can be concluded from the influence of introducing a waiting period between the ion implantation and subsequent magnetron sputtering.

CONCLUSION

In our search for processes which give rise to an increase in ATV in reactive sputtering, at least two such mechanisms could be identified. It was shown that in the system Al/O_2, chemisorption on the target surface is responsible for such an increase in ATV. By correlating the ATV with the effective covered fraction of the target by chemisorption θ^*_{tc} minus the fraction θ_{ti} of the target surface converted into compound by subplantation of reaction gas, a fairly good agreement between the experimental observed variation of the ATV versus the flow of reaction gas and the calculated values is obtained. Comparing the influence of chemisorption with the influence of implantation shows that even in systems such as Al/O_2 sputtering, in which poisoning has been attributed traditionally to chemisorption, this effect alone is not able to describe the observed ATV values during poisoning. Indeed, even in those systems, chemisorption is essentially a trigger for the real poisoning mechanism, namely, reactive subplantation. In the system Ag/N_2, more precisely by implanting N_2^+ ions in a silver target, it was possible to prove that the injected nitrogen does not react with the Ag lattice while giving rise to an increase in ATV. It must be concluded that the injected nitrogen remains dissolved in the Ag lattice and reduces the ion induced secondary electron emission of the target which in turn leads to an increase in ATV. The process by which dissolved nitrogen reduces the ISEE still remains unknown.

APPENDIX

The relevant equations [9] describing the extended model are: The symbols are defined as follows:

- θ_{tc}: fraction of target surface covered by chemisorption
- θ_{ti}: fraction of target surface that has reacted with subplanted reactive atoms or ions under the formation of compound
- n: concentration of subplanted reactive gas atoms before reaction and diffusion (m^{-3})
- n_o: target density (m^{-3})
- α_{ti}: reaction probability of a subplanted atom with a target lattice atom
- a: number of reactive gas atoms needed to form one molecule of the compound
- f: mole fraction of the reactive gas in the gas phase
- Y: sputter yield of the target
- N: concentration of subplanted and non reacted ions in the target (m^{-3})
- N_{max}: Maximum value of N (m^{-3})
- γ_M: sputter yield of the target material
- γ_R: sputter yield of the compound
- α_{tc}: sticking coefficient of reactive gas molecules on the target
- F: flux of reactive gas molecules towards the target (at. $m^{-2}.s^{-1}$)
- I: discharge current density (ions $m^{-2}.s^{-1}$)
- β: probability that a subplanted reactive atom remains non reached in the target
- P_T: total pressure (P_a)
- P: partial pressure of reaction gas (P_a)

Figure A1 shows the flow chart for calculating all relevant quantities. The numbers between brackets refer to the corresponding equations. Bold lines show that part of the flow chart that is directly accessible from the experimental quantities I, P and P_T. It allows calculating F, f and θ_{tc}. Thin lines show the iterative part of the flow chart. Starting with a best guess for n, it allows calculating a new value of n. Feeding back this value (hatched line) starts an iterative process until initial and final values of n are converging. This gives calculated values for θ_{ti}, θ_{csc} and N.

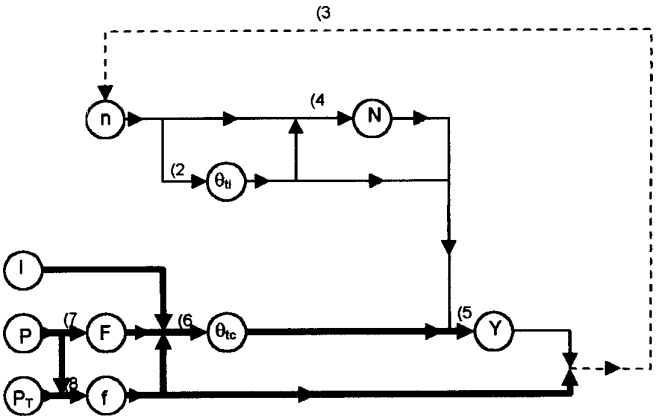

Figure A1

ACKNOWLEDGEMENTS

The authors are indebted to the Bekaert Company for the financial support for their research.

REFERENCES

1. S. Berg, H.-O Blom, T. Larsson, C. Nender, "Modelling of reactive sputtering of copound materials", *J. Vac. Sci. Technol.*, A5 (2), 202, 1987.

2. D. Depla, R. De Gryse, "Influence of oxygen addition on the target voltage during reactive sputtering of aluminium", *Plasma Sources Sci. Technol.*, 10, 547, 2001.

3. D. Depla, A. Colpaert, K. Eufinger, A. Segers, J. Haemers, R. De Gryse, "Target voltage behaviour during DC sputtering of silicon in an argon/nitrogen mixture", *Vacuum"*, 66, 9, 2002.

4. J.F. Ziegler, J.P. Biersac, L. Littmark, "The stopping and Range of Ions in Solids", *Pergamon,* New York, 1985.

5. D. Depla, R. De Gryse, "Cross section for removing

chemisorbed oxygen from an aluminium target by sputtering", *J. Vac. Sci. Technol.*, A20 (2), 521, 2002.

6. E. Kusano, S. Baba, A. Kinbare, "An approach to estimate gettering effects in TiO_2 reactive sputtering processes", *J. Vac. Sci. Technol.*, A10 (4), 1696, 1992.

7. L. Pekker, "Plasma chemistry model of DC magnetron reactive sputtering in ArO2 gas mixture", *Thin Solid Films*, 312, 341, 1998.

8. R. De Gryse, D. Depla, J. Haemers, "Gas implantation in sputter targets as a factor determining the target voltage in reactive sputtering," *46th Annual Technical Conference Proceedings of the Society of Vacuum Coaters*, p. 615, 2003.

9. D. Depla, R. De Gryse, "Target poisoning during reactive magnetron sputtering: Part II: the influence of chemisorption and gettering", *Surface & Coatings Technology"* 183, 190, 2004.

10. J.C. Ingram, K.W. Nebesny, J.E. Pemberton, "Optical-properties of selected 1st-row transition-metals determined by reflection electron-energy loss spectroscopy", *Appl. Surf. Sci*., 45, 247, 1990.

11. M. Jo, "Relation between the shape of measured loss function and the resolution of the XPS spectrum", *Appl. Surf. Sci*, 145, 49,1999

12. I. Gouzman, R. Brener, A. Hoffman, "Electron spectroscopic study of C-N bond formation by low-energy nitrogen ion implantation of graphite and diamond surfaces", *J. Vac. Sci. Technol A*, 17, 411, 1999.

13. D. Depla, J. Haemers, R. De Gryse, "Target surface condition during reactive glow discharge sputtering of copper", *Plasma Sources Sci. Technol*., 11, 91 2002.

14. J.C.C. Tsai, J.M. Morabito, "Mechanism of simultaneous implantation and sputtering by high-energy oxygen ions during Secondary Ion Mass-Spectrometry (SIMS) Analysis", *Surf. Sci.*, 44, 247, 1974.

15. H. Liebl, "Secondary-Ion Mass-Spectrometry And Its Use In Depth Profiling", *J. Vac. Sci. Technol*, 12, 385, 1975.